A Regularized Optimization Approach for AM-FM Reconstructions

Paul Rodríguez
Department of Electrical Engineering
Pontificia Universidad Católica del Perú
Lima, Peru
Email: prodrig@pucp.edu.pe

Victor Murray and Marios S. Pattichis
Department of Electrical and Computer Engineering
University of New Mexico
Albuquerque, NM
Email: vmurray@ieee.org, pattichis@ece.unm.edu

***Abstract*— The AM-FM Dominant and Channelized Component Analysis (DCA and CCA respectively) [1], consist of applying a filter bank to the Hilbert-tranformed image, and then proceeding with the AM-FM demodulation of each band-pass filtered image. Whereas AM-FM reconstructions based on the CCA use a reasonably small number of locally coherent components, those based on the DCA only use one component: the estimates from the channel with the maximum amplitude estimate. Both types of reconstructions are known to produce noticeable visual artifacts.**

We propose a method, based on a regularized optimization of the estimates from the CCA, which attains a small number of locally coherent components and simultaneously enforces a piece-wise smooth constrain for the amplitude functions. Moreover, this method offers high quality reconstructions when compared to standard CCA and DCA reconstructions and state of the art techniques [2].

I. Introduction

The AM-FM representation of images allows us to model non-stationary image content in terms of amplitude and phase functions using

$$b(\xi) \quad = \quad \sum_{n=1}^{L} a_n(\xi) \cos(\varphi_n(\xi)) \qquad (1)$$

where $b(\xi) : \mathbb{R}^2 \to \mathbb{R}$ is the input image, $\xi = (\xi_1, \xi_2) \in \mathbb{R}^2$, $M \in \mathbb{N}$, $a_n : \mathbb{R}^2 \to [0, \infty)$ and $\varphi_n : \mathbb{R}^2 \to \mathbb{R}$. The interpretation of (1) suggests that the L AM-FM component images, $a_n(\xi) \cdot \cos(\varphi_n(\xi))$, model the essential image modulation structure, the amplitude functions $a_n(\xi)$ embed the contribution (intensity in this context) of an image's region, and the FM components $\cos(\varphi_n(\xi))$ capture fast-changing spatial variability in image intensity.

It is important to point out that (1) can also be interpreted as a separation of texture (FM components $\cos(\varphi_n(\xi))$) from piecewise smooth content (amplitude functions $a_n(\xi)$) in an image [3].

The AM-FM Dominant and Channelized Component Analysis (DCA and CCA respectively), described in [1], [4], consist on applying a collection of band-pass filters (filter bank) to the original image, and then proceed with the AM-FM demodulation of each band-pass filtered image, which implies the estimation of:

- the instantaneous amplitude (IA) functions $a_n(\xi)$,
- the instantaneous phase (IP) functions $\varphi_n(\xi)$, and
- the instantaneous frequency (IF) vector functions $\omega_n(\xi) = \nabla\varphi_n(\xi)$.

Whereas the CCA's goal is usually to obtain a reasonably small number of locally coherent components (modeling the input image as in (1)), the DCA goes on and selects the estimates from the channel with the maximum amplitude estimate using just one component (the dominant) to model the input image.

In this work we hypothesise that the minimum of

$$J(\mathbf{a}, \boldsymbol{\zeta}) = \frac{1}{p}\|f(\mathbf{a}, \boldsymbol{\zeta}) - \mathbf{b}\|_p^p + \lambda_a T(\mathbf{a}) + \lambda_\zeta \|\boldsymbol{\zeta}\|_1, \;\; \text{s.t. } \mathbf{a} \geq 0 \;, |\boldsymbol{\zeta}| \leq 1 \qquad (2)$$

attains a small number of locally coherent components and simultaneously enforces a piecewise smooth constrain for $a_n(\xi)$. We employ the following notation:

- the 1D vectors $\mathbf{a}_n$, $\boldsymbol{\zeta}_n$ and $\mathbf{b}$ represent the 2D IA function $a_n(\xi)$, the
 2D function $\cos(\varphi_n(\xi))$ and the (grayscale) image $b(\xi)$,
- $\mathbf{a} = [\mathbf{a}_1^T, \mathbf{a}_2^T, .., \mathbf{a}_L^T]^T$, $\boldsymbol{\zeta} = [\boldsymbol{\zeta}_1^T, \boldsymbol{\zeta}_2^T, .., \boldsymbol{\zeta}_L^T]^T$,
- $f(\mathbf{a}, \boldsymbol{\zeta}) = \sum_{n=1}^{L} \mathrm{diag}(\mathbf{a}_n) * \boldsymbol{\zeta}_n$ (see (1)),
- $T(\mathbf{a}) = \frac{1}{q}\left\| \sqrt{\sum_n (D_x\mathbf{a}_n)^2 + (D_y\mathbf{a}_n)^2} \right\|_q^q$ is the TV regularization ge-
 neralization to vector-valued images with coupled channels [5], and
- D_x and D_y represent horizontal and vertical discrete derivative op-
 erators respectively.

II. Regularized optimization for AM-FM reconstructions

The motivation for (2) is to enforce two constrains in the AM-FM reconstruction: we want (i) a small number of locally coherent components and (ii) a piecewise smooth constrain for the amplitude functions $a_n(\xi)$ in (1).

The functional $J(\mathbf{a}, \boldsymbol{\zeta})$ (see (2)) is convex in $\mathbf{a}$ or in $\boldsymbol{\zeta}$, but it is not necesarilly convex in both variables together. Somehow similar problems have been previously described (for instance see [3], [6]) for which numerical solutions aim to find a local minima by alternating updates for each independant variable.

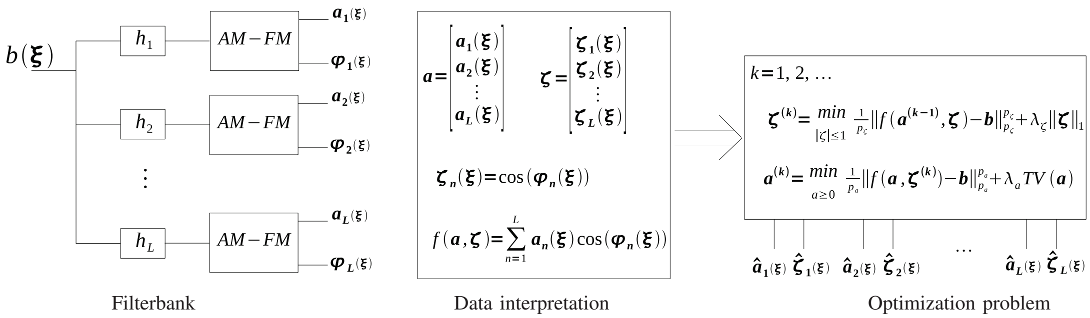

Fig. 1. Regularized optimization for AM-FM reconstructions. In this figure, we depict the solution to the minimization problem described in (2), which we hypothesise attains a small number of locally coherent components and simultaneously enforces a piecewise smooth constrain for the amplitude functions. The resulting amplitude and (cosine of the) phase functions $\hat{\mathbf{a}}_n(\xi)$ and $\hat{\zeta}_n(\xi)$ maybe be used to reconstruct the input image via the CCA or DCA method. See Figure 2 for experimental results.

In Algorithm 1 we summarized our optimization procedure, where (3) may be solved using the ideas exposed in [7], which is based on the non-negative quadratic programming optimization algorithm [8] and on the FOCUSS algorithm [9], and (4) may be solved via the vv-IRN-NQP algorithm [10], which is based on [8] and on the iteratively reweighted norm (IRN) algorithm for vector-valued images [11].

for $k = 1,\ 2,\ ..$

$$\boldsymbol{\zeta}^{(k)} = \min_{|\boldsymbol{\zeta}|\le 1} \ \tfrac{1}{p_\zeta}\|f(\mathbf{a}^{(k-1)},\boldsymbol{\zeta})-\mathbf{b}\|_{p_\zeta}^{p_\zeta} + \lambda_\zeta\|\boldsymbol{\zeta}\|_1 \quad (3)$$

$$\mathbf{a}^{(k)} = \min_{\mathbf{a}\ge 0} \ \tfrac{1}{p_a}\|f(\mathbf{a},\boldsymbol{\zeta}^{(k)})-\mathbf{b}\|_{p_a}^{p_a} + \lambda_a T(\mathbf{a}) \quad (4)$$

Algorithm 1: Proposed algorithm to solve (2). $\mathbf{a}^{(0)}$ is the IA estimation from CCA.

We must stress that the proposed procedure is strongly dependant on the accuracy of the initial IA estimates. In this work, for the initial IA estimates, we prefer the Quasi-Local method [12] over the Quasi-Eigen Aproximation [1] method (based on the analytic signal) because the IA estimates from first method are less sensitive to perturbations (noise) than the IA estimates of the latter [13].

III. Preliminary Experimental Results

The performance (image reconstruction quality) of our proposed method was compared with that of several alternative approaches: CCA, DCA, and the methods proposed in [2], [14]: LESHA, LESHAL and MULTILES. For the CCA and DCA approaches, the IA was computed via Quasi-Local (QLM) method [12] and the IP via the Quasi-Eigen Aproximation (QEA) method [1], whereas for the LESHA, LESHAL and MULTILES methods the IA and IP estimations are based on the QEA method (see [2], [14] for details). For all cases the image reconstruction quality of our proposed method was superior than that of the other considered methods.

We use a separable filterbank covering the whole frequency spectrum consisting of one low-pass and one high-pass filter. We notice that each separable channel filter has support over four quadrants. Here, to maintain support over only two quadrants (needed for the QEA method), we used FFT prefiltering to remove support in two quadrants (as needed). The filters were designed using an optimal min-max, equiripple approach. Passband ripple was set at 0.017dB and the stopband attenuation was set to 66.02dB.

The test images are the synthetic image “Radial Chirp” (see Figure 2.(a)) and the “Lena” and “Barbara” images; all images are 512×512 pixel. All simulations have been carried out using Matlab-only code on a 1.83GHz Intel Dual core CPU (L2: 2048K, RAM: 4G).

	SNR (dB)					
Image	DCA	CCA	LESHA	LESHAL	MULTILES	(2) + DCA
Radial Chirp	6.51 (14.43)*	3.21 (-2.63)*	0.51	13.56	13.56	15.41
Barbara	0.92 (7.69)*	1.15 (9.76)*	10.48	12.69	12.69	22.39
Lena	0.83 (5.38)*	0.46 (6.58)*	14.97	15.16	15.16	24.40

TABLE I

Reconstruction performance comparison between the DCA, CCA, LESHA [2], LESHAL [2] and MULTILES [2] and the proposed method: (2)+DCA (or DCA applied to $\hat{\mathbf{a}}$ and $\hat{\boldsymbol{\zeta}}$, see Figure 1) on the “Radial Chirp”, “Barbara” and “Lena” test images. Values marked with ()* indicates that the reconstructed image has been normalized.

	SSIM index [15]					
Image	DCA	CCA	LESHA	LESHAL	MULTILES	(2) + DCA
Radial Chirp	0.929	0.766	0.144	0.815	0.815	0.978
Barbara	0.730	0.544	0.619	0.656	0.656	0.987
Lena	0.623	0.378	0.731	0.731	0.731	0.962

TABLE II

Reconstruction performance comparison using the SSIM index [15] as a metric for the same setup of Table I

In Tables I and II we use the SNR and SSIM index [15] between the original image and the reconstructed image as a measure of the image reconstruction quality, and present the performance results between the afore mentioned methods

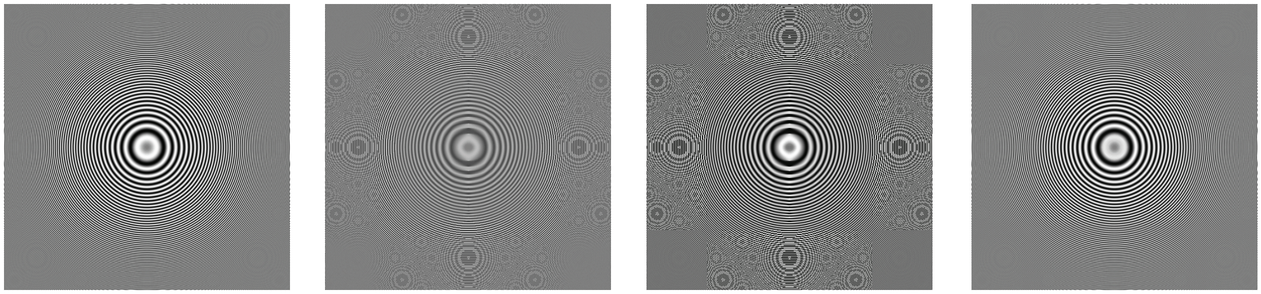

(a) Input image "Radial Chirp" (b) Reconstructed via CCA. (c) Reconstructed via DCA. (d) Reconstructed via DCA applied to $\hat{\mathbf{a}}$ and $\hat{\boldsymbol{\zeta}}$ (see Figure 1).

(e) Input image "Barbara" (f) Reconstructed via CCA. (g) Reconstructed via DCA. (h) Reconstructed via DCA applied to $\hat{\mathbf{a}}$ and $\hat{\boldsymbol{\zeta}}$ (see Figure 1).

Fig. 2. Test images "Radial Chirp" and "Barbara", and their AM-FM reconstruction versions

and compared it with that of our proposed method. For all cases our method has superior performance, specially for the "Barbara" and "Lena" images where our proposed method attains very high SNR (≥ 22 dB) compared with the modest SNR of all other methods (≤ 15.2 dB)

IV. Conclusions

The proposed method for AM-FM reconstructions offers high quality reconstructions, both visually and quantitatively. Moreover, the experimental results gives support to our hypothesis: the minimum of (2) attains a small number of locally coherent components and simultaneously enforces a piecewise smooth constrain for $a_n(\xi)$.

On-going work is focused on theoretical implications of (2).

References

[1] J. P. Havlicek, D. S. Harding, and A. C. Bovik, "Multidimensional quasi-eigenfunction approximations and multicomponent am-fm models," *IEEE TIP*, vol. 9, no. 2, pp. 227–242, 2000.

[2] V. Murray, P. Rodríguez, and M. Pattichis, "Multi-scale AM-FM demodulation and reconstruction methods with improved accuracy," *IEEE TIP*, vol. 19, no. 6, pp. 1138–1152, 2010.

[3] J. L. Starck, M. Elad, and D. L. Donoho, "Image decomposition via the combination of sparse representations and a variational approach," *IEEE TIP*, vol. 14, pp. 1570–1582, 2005.

[4] J. P. Havlicek, "AM-FM Image Models," PhD thesis, The University of Texas at Austin, 1996.

[5] A. Bonnet, "On the regularity of edges in image segmentation," *Annales de l'institut Henri Poincaré (C) Analyse non linéaire*, vol. 13, no. 4, pp. 485–528, 1996.

[6] Daniel D. Lee and H. Sebastian Seung, "Algorithms for non-negative matrix factorization," in *Proceedings of the Conference on Neural Information Processing Systems (NIPS)*, 2000, pp. 556–562.

[7] Paul D. O'Grady and Scott T. Rickard, "Recovery of non-negative signals from compressively sampled observations via non-negative quadratic programming," in *Proceedings Signal Processing with Adaptive Sparse Structured Representations*, Saint-Malo, France, Apr. 2009.

[8] Fei Sha, Yuanqing Lin, Lawrence K. Saul, and Daniel D. Lee, "Multiplicative updates for nonnegative quadratic programming," *Neural Comput.*, vol. 19, no. 8, pp. 2004–2031, 2007.

[9] Bhaskar D. Rao and Kenneth Kreutz-Delgado, "An affine scaling methodology for best basis selection," *IEEE TSP*, vol. 47, no. 1, pp. 187–200, Jan. 1999.

[10] Paul Rodríguez, "A non-negative quadratic programming approach to minimize the generalized vector-valued total variation functional," Acepted to European Signal Processing Conference, Aug. 2010.

[11] Paul Rodríguez and Brendt Wohlberg, "A generalized vector-valued total variation algorithm," in *Proceedings of the International Conference on Image Processing (ICIP)*, Cairo, Egypt, Nov. 2009, pp. 1309–1312.

[12] G. Girolami and D. Vakman, "Instantaneous frequency estimation and measurement: a quasi-local method," *Measurement Science Technology*, vol. 13, pp. 909–917, june 2002.

[13] Paul Rodríguez, "Fast and Accurate AM-FM Demodulation of Digital Images with Applications," PhD thesis, University of New Mexico (UNM) Albquerque, NM, USA, 2005.

[14] Victor Manuel Murray Herrera, *AM-FM Methods for Image and Video Processing*, Ph.D. thesis, University of New Mexico, 2008.

[15] Z. Wang, A. Bovik, H. Sheikh, and E. Simoncelli, "Perceptual image quality assessment: From error visibility to structural similarity," *IEEE TIP*, vol. 13, no. 4, pp. 600–612, April 2004.